Available online at www.CivileJournal.org

Civil Engineering Journal

(E-ISSN: 2476-3055; ISSN: 2676-6957)

Vol. 11, No. 06, June, 2025

Axial Compression Behavior of Concrete-Encased CFST Columns

Raad Abdulkhudhur [1], Mohammed Elwi [1], Hussein Al-Quraishi [1*]

[1] *Department of Civil Engineering, University of Technology, Baghdad, Iraq.*

Received 04 February 2025; Revised 09 May 2025; Accepted 14 May 2025; Published 01 June 2025

Abstract

Composite construction known as concrete-encased CFST is an outer covering of concrete surrounding a steel tube filled with concrete. It is employed as a structural member in multi-story buildings, large structures, bridges, and underground subway systems. Most of the literature deals with steel tubes filled with core concrete or concrete-encased steel tubes filled with core concrete with main reinforcement, but in the present study, CFST is used as conventional reinforcement. Therefore, five concrete-encased CFST columns and one normal reinforced concrete column were loaded axially. Variables were effects of CFST, percentage of steel tubes, outer concrete compressive strength, compressive strength of steel tube concrete, and ratio of unfilled steel tubes. The experimental test result of the reference concrete-encased CFST ultimate axial compression strength showed 65.1% strength of a conventional column. An increase in the ratio of CFST from 6.8% to 10.2% enhanced ultimate axial compression by 19.2% compared to the reference concrete-encased CFST column. Furthermore, a rise in the outer compression strength of the outer concrete from 15 MPa to 20 MPa resulted in an increase of 14.94% in ultimate axially compression loads. An increase of concrete compression strength within the steel tubes from 35 MPa to 45 MPa resulted in a slight increase of 0.62% in the ultimate load. The 16.8% reduction in the ultimate load, however, was due to the presence of a hollow steel tube inside the concrete-filled CFST. The validated finite element model was therefore employed to examine the effect of different parameters that affect the concrete column using a parametric study.

Keywords: Concrete Filled Steel Tube; Short Column; Axial Strength; CFST.

1. Introduction

Concrete-encased concrete-filled steel tube (CFST) related to a composite structural member composed of a concrete-filled steel tube (CFST) covered with an outer concrete. Concrete-encased CFST is more ductile than ordinary reinforced concrete members. Han & An (2014) [1] tested the axial compression behavior of concrete-encased CFST stub columns. FEA models are widely applicable for the analysis of composite columns of such a kind. Material nonlinear behavior and interaction between concrete-steel tubes are present in this method. The experimental evidence supports the FEA modeling, and it is utilized to investigate systematically load-versus-deformation interactions in concrete-encased CFST stub columns. The research compares interaction between the steel tube, inner concrete, and outer concrete in CFST. Concrete-encased CFST, normal CFST, and RC columns are also contrasted among themselves. FEA modeling is subsequently used in performing parametric analysis.

An et al. (2014) [2] conducted theoretical analysis on the behavior of concrete-encased CFST box columns under eccentric axial loading. The study employed finite element analysis (FEA) in the composite column analysis and

* Corresponding author: hussein.a.alquraishi@uotechnology.edu.iq

http://dx.doi.org/10.28991/CEJ-2025-011-06-05

validated its accuracy through comparison with test results. Further, the study addresses the behavior of composite materials based on observation of the mid-height deflection against applied load. The moment magnification approach was also found to be appropriate, yielding an acceptable approximation. Further, with the rise in the load eccentricity to sectional width ratio (e/B), the contribution of the inner CFST section in the load diminishes, and the composite column's moment contribution rises at the ultimate load. Concrete enclosure CFST box columns are stronger and stiffer than CFST built-up columns and reinforced concrete box columns. Strength and stiffness are controlled by concrete area, steel area, and concrete strength for compression-controlled composite columns. Steel area is the controlling factor for strength and stiffness for tension-controlled failure columns. Sectional characteristic variations do not significantly influence failure modes such as compression and tensile failure. The force ratio (e/B) and the slenderness parameter (λ) are the most influential parameters on the failure mode. Ali et al. (2013) [3] studied the circular column filled with a steel tube applied to concentric loading till failure. SCC was used as a filling in an effort to improve core homogeneity and avoid segregation issues. Six specimens of different lengths (between 0.4 m and 1.5 m), 160 mm in diameter, and 2.8 mm thick were tested. Deformation and strength of variant slender ratios were obtained. Compressive strength of concrete-filled steel tube (CFST) columns from experimental evidence indicates that their slenderness ratio is responsible mainly for this property. Thin columns fail primarily in general buckling, and short columns fail primarily in local buckling and crushing modes.

An & Han (2014) [4] studied the behavior of concrete-encased CFST columns under combined compression and bending. A finite-element analysis model was used to study the composite column response, with calculated results exhibiting excellent agreement with test results in failure modes, load-deformation behaviors, and ultimate load. The topic includes general modes of failure, the entire behavior of the load-lateral deflection curve, the transfer of load within the outer concrete and inner CFST, and concrete-steel tube contact stress. The effects of loading direction and slender ratio on composite column behavior are also studied in the paper. The impact of various parameters like concrete strength and steel strength, CFST steel ratio, ratio of longitudinal bars, and CFST size on the capacity of the section of concrete-encased CFST columns is investigated based on the finite element model. A simplified model must be constructed for the calculation of the sectional capacity of the concrete-encased CFST columns under the combined compression and bending. Chen et al. (2019) [5] tested the structural performance of the concrete-encased CFST box stub columns axially loaded. The column consists of an external reinforced concrete (RC) box column that embeds six CFST members. Eight axial compressions were tested on concrete-filled CFST box samples to investigate their structural behavior. Besides, a finite element analysis (FEA) model was established for comparative investigation of such composite column behavior. Material nonlinearities and steel-concrete tube interaction were considered in the analysis. The FEA model was validated and used to conduct a detailed load-deformation response analysis. Typical failure modes, structure load and stress distribution, and steel and concrete tube contact stresses were provided by the research. Parametric analysis was conducted with a view to study the effect of material and geometrical model on the compressive concrete-encased CFST box member. Initial stiffness and compressive strength of a concrete-encased CFST box column under compression loading were determined based on a simplified model.

Ali & Abbas (2021) [6] studied the behavior of box concrete-filled steel tube (CFST) columns from the point of view of the confinement effect. The ultimate strength of CFST columns is hard to analyze because confined pressure influences them. Based on a database of 188 tested columns, two types of predictive equations—simplified and modified—were formulated to estimate their structural performance. The predictive equations are applied in forecasting the ultimate strength of box composite columns of varied configurations and material constituents. Other code systems and equations that evolved earlier were applied in checking and establishing reliability. Axial load-shortening behavior of composite columns has been examined based on a proposed model of confined concrete using finite element analysis. The model was then compared to experimental data and found to be in close accord with prediction and experiment. The verified formulas and exact model provided results found to be congruent with experiment results. Al-Abbas et al. (2023) [7] performed the research on high-deformation composite concrete-filled tubular steel (CFT) members because of the found confined and constrained interaction of the steel and concrete tubes. These composite columns have wide applications as tall building structural columns and bridge pier columns with greater strength for the same column size. The present research endeavored to pursue RPC-filled steel tube column axial compression tests. The experiment was performed on square, rectangular, and circular column test pieces with varied lengths to diameters and various compressive strengths of RPC. There were five columns in the first experiment and seven columns with dimensions of 750, 600, and 450 mm and compressive strengths of 54 MPa and 92 MPa in the second and third experiments. In calculating the ultimate failure load for the columns, a new equation was formulated taking into account column dimensions, steel-to-concrete ratio, steel yield, and concrete compressive strength. A comparison was conducted between the established model and experimental tests and design equations in other structural building codes in order to cross-validate.

Abdulkhudhur et al. (2024) [8] performed numerical analysis of concrete-encased concrete-filled steel tube (CFST) columns and examined different parameters influencing their axial compression strength. The study was performed for the effect of outer normal compressive strength of concrete, core self-compacting compressive strength of steel tubes in

concrete, steel tube diameter, yielding stress of steel tubes, and ratio of steel fibers in outer normal concrete. It came up with results that indicate the outermost controlling parameters of CFST column axial compressive strength to be steel tube diameter, steel tube yield stress, and outer concrete compressive strength.

In summary, most of the literature deals with steel tubes filled with core concrete or concrete-encased steel tubes filled with core concrete with main reinforcement, but in the present study, CFST is used as conventional reinforcement to find the short column axial compression strength. Also, it employs both experimental and numerical simulation to find the most influential factors on the axial compression strength of concrete-encased CFST columns, utilizing a power function to quantify their influence.

2. Experimental Program

2.1. Specimens Details

A conventional column strengthened with ordinary steel bars had a cross-section of 170 × 170 × 910 mm, and five concrete-encased CFST columns were constructed. During the design phase of the experimental program, the research mainly concentrated on major variables such as the CFST ratio, the outer concrete compressive strength, the steel tube compressive strength of concrete, and the unfilled steel tubes. Table 1 outlines the experimental program construction and the variables considered for this study. The steel pipes of 25 mm diameter and 1.8 mm thickness used in the current study possess a yield strength of 456 MPa and an ultimate tensile strength of 492 MPa. The deformed 25 mm diameter steel bars possess a yield strength of 581.74 MPa and an ultimate tensile strength of 681.31 MPa. Meanwhile, the yield strength and ultimate tensile strength of 10 mm diameter stirrups are 555 and 651.8 MPa, respectively. The geometric arrangement of CFSTs and ties of test specimens is shown in Figure 1.

Table 1. Experimental program and variables for concrete-encased CFST columns

Symbol	Variable	Compressive strength of outer concrete fc (MPa)	Compressive strength of concrete in steel tube fc (MPa)	Ratio of CFST%
C1	Conventional	15	---	---
C2	Reference	15	35	6.8
C3	Ratio of CFST	15	35	10.2
C4	Compressive strength of outer concrete	20	35	6.8
C5	Compressive strength of concrete in steel tube	15	45	6.8
C6	Unfilled steel tube	15	---	6.8

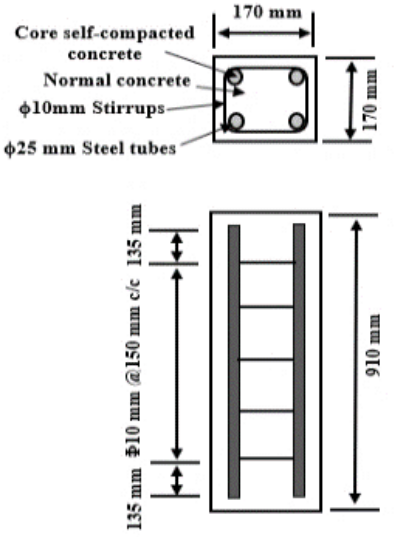

Figure 1. Concrete-encased CFST column

2.2. Mix Proportions

Test samples were cast with Portland cement Type I, specific gravity 3.15 g/cm³. Fine aggregate was Zone 2 according to a grading test, and the natural coarse aggregate was of particle size up to 5–14 mm. Silica fume, specific gravity 2.2 g/cm³, was added to replace 10% of the cement weight to improve the concrete mix. In addition, Viscocrete-905, 1.065 g/cm³ specific gravity high-range water-reducing admixture, was utilized. The admixture was utilized to reduce the water-cement ratio and consequently the strength of concrete [9-11].

Experimental concrete mixes for concrete-encased columns are two in number: one for the preparation of self-compacting concrete filled in a steel tube, and another for the preparation of normal-strength concrete encased CFSTs on the outside. Self-compacting concrete mixes have been prepared to attain a compressive strength of 35, 45, and 55 MPa, whereas outer normal concrete mixes have been formulated to attain a compressive strength of 15, 20, and 25 MPa at 28 days, as indicated in Table 2.

Table 2. Mix proportions of self-compacted (SCC) and normal concrete

Mix type	Cement (kg/m^3)	Gravel (kg/m^3)	Sand (kg/m^3)	Silica fume (kg/m^3)	Water (kg/m^3)	w/c	Superplasticizer (%)	Compressive strength of cylinders (MPa)
SCC1	420	841	841	42	218	0.52	1.11	35
SCC2	520	800	800	52	200	0.38	1.28	45
SCC3	550	833	833	55	165	0.30	1.82	55
NC1	311	912	892	0	200	0.643	0	15
NC2	350	912	853	0	200	0.571	0	20
NC3	399	912	803	0	200	0.501	0	25

2.3. Testing of Fresh SCC

Three principal tests were conducted to determine the characteristics of SCC, like slump flow, L-box, and V-funnel, according to EFNARC (2002) [12].

2.3.1. Slump Flow and T500 Tests

The slump flow test provides a quick means of measuring the flowability of SCC by its horizontal flow diameter for filling capacity and T500 time for viscosity. It also helps in measuring resistance to segregation. The test can easily be performed on a work site using an inverting or vertical cone Abram. The process is a procedure of concreting of the cone with SCC onto a leveled flat steel plate (900 × 900 mm) and raising it 15 to 30 mm in 2 to 4 seconds so that gravity can spread the mix. The acceptance criteria must meet BS EN 12350-8 [13].

2.3.2. L-Box Test

The L-box test is a test used to determine the passing and filling amount of self-compacting concrete (SCC) with respect to its ability to pass through rebar without clogging or segregating. The L-box apparatus consists of a vertical and horizontal compartment divided by a three-bar gap. The vertical compartment is filled, and subsequently, the gate is opened to allow SCC to flow into the horizontal compartment past the rebar obstructions. The initial (H1) and final (H2) heights of the concrete at the start and end of the horizontal section are measured, and the ratio of H2 to H1 (typically 0.8–1) indicates the filling capacity. The passing ability is determined by direct visual inspection of the concrete in the rebar area. The test must meet the BS EN 12350-10 [14].

2.3.3. V- Funnel Test

The V-funnel test is utilized for ascertaining the filling capacity and viscosity of self-compacting concrete (SCC). In the test, 0.012 m^3 of concrete is filled in the funnel, and the gate is shut. Upon opening the gate, SCC flows into a container positioned below it, and the total flow time is measured to attain concrete viscosity. The test must satisfy the acceptance criteria as given in BS EN 12350-9 [15].

2.4. Steel and Concrete Strain Gauge

A single steel strain gauge is mounted on the half-length of the steel tube, and two concrete strain gauges are mounted horizontally at the center of the column on two adjacent surfaces.

2.5. Linear Variable Differential Transformer (LVDT)

Three LVDTs were installed in key positions for measuring axial shortening and lateral deformation of CFST columns. A single linear variable differential transformer (LVDT) was installed on the base plate for loading to measure column axial shortening. Two LVDTs were installed at specific points on adjacent faces in the middle region of each specimen's length to measure lateral deformation.

2.6. Test Setup

The column specimens were side-supported at their top and bottom by bolted steel boxes, which were fabricated from 6 mm-thick steel plates to prevent failure in bearing. Column stiffening was done at both ends by 30 mm-thick

steel plates for proper axial load distribution. LVDTs were provided in their respective positions for axial shortening and lateral deformation measurement. CFST columns cast in concrete were subjected to a test on a hydraulic testing machine (AVERY) with a capacity of 2500 kN and with an ability to control the applied load accurately. The test setup, as shown in Figure 2, was carried out at the University of Technology Laboratory.

Figure 2. Testing the apparatus and instrumentation for concrete-encased CFST column

Three locations were particularly identified to be employed for the installation of LVDT to make measurements of the axial shortening and lateral deflection of CFST columns. There was only one loading base plate mounting point for the installation of a single linear variable differential transformer (LVDT) utilized to get a reading for the column's axial shortening. Two LVDTs were also positioned on adjacent surfaces at the half-length of each specimen to track lateral deformation, as shown in Figure 2.

Steel rings were positioned at column ends before the test in order to prevent bearing failure. The LVDTs and load applied were calibrated and set up before testing. Vertical load was applied at the top of the columns utilizing a load control system at the rate of 1 kN/sec. All specimens were loaded until failure.

3. Experimental Results

The test results take into account the effect of various variables on axial compression load, including the development of CFST, steel tube ratio, outer concrete compressive strength, compressive strength of inner concrete in steel tubes, and the influence of steel tubes without filling. The comparison study of test outcomes is presented in Table 3, considering ultimate axial compression load, axial shortening, and lateral displacement. The reference column (C2) is compared with columns (C1, C3, C4, C5, and C6) based on study variables.

Table 3. Information on experimental results for concrete-encased CFST columns

Specimens	Variables	Ratio of CFST %	Compressive strength of outer concrete fc (MPa)	Compressive strength of concrete in FST fc (MPa)	Ultimate load (P_U) kN	Axial shortening (mm)
C1	Conventional	---	15	---	1489.4	1.74
C2	Reference	6.8	15	35	969.5	2.40
C3	Ratio of CFST	10.2	15	35	1155.6	1.94
C4	Compressive strength of outer concrete	6.8	20	35	1114.3	2.04
C5	Compressive strength of concrete in FST	6.8	15	45	975.5	2.38
C6	Unfilled steel tube	6.8	15	---	806.7	2.80

From Table 3 and Figure 3, the following can be observed:

- The results show that the strength of the reference column (C2) to sustain the ultimate load is 65.1% of the conventional column. This is due to the increase in axial stiffness of CFST compared with conventional rebar. The axial shortening of the conventional column decreases by 27.5% compared with (C2).
- It is found that the ultimate axial compression load of the column (C3) increases by 19.2% as a result of the increased number of steel tubes (10.2% ratio of CFST). This is due to a stronger and more resilient structural system. Also, column axial shortening lowers by 19.2%.

- Increasing the outer compressive strength from 15 MPa to 20 MPa at the column (C4) increases the ultimate load by 15% compared to column C2, which has an outer compressive strength of concrete equal to 15 MPa. This is due to the higher fracture energy of concrete with compressive strength increasing. Additionally, the axial shortening of the column (C4) decreased by 15% compared with the column (C2).
- Increasing the concrete compressive strength on the inner steel tubes from 35 MPa to 45 MPa leads to increasing the ultimate load by 0.62% compared to column (C2). This is due to an increase in the fractured energy of confined concrete. Additionally, the axial shortening of the column (C5) decreased by 0.83%.
- The unfilled steel tubes for column (C6) had a 16.8% lower ultimate axial compression load than the reference column (C2), which had 35 MPa self-compacted concrete. This is due to the reduced axial stiffness of the FS tube compared with CFST. The column axial shortening increased by 16.7% compared to column (C2).

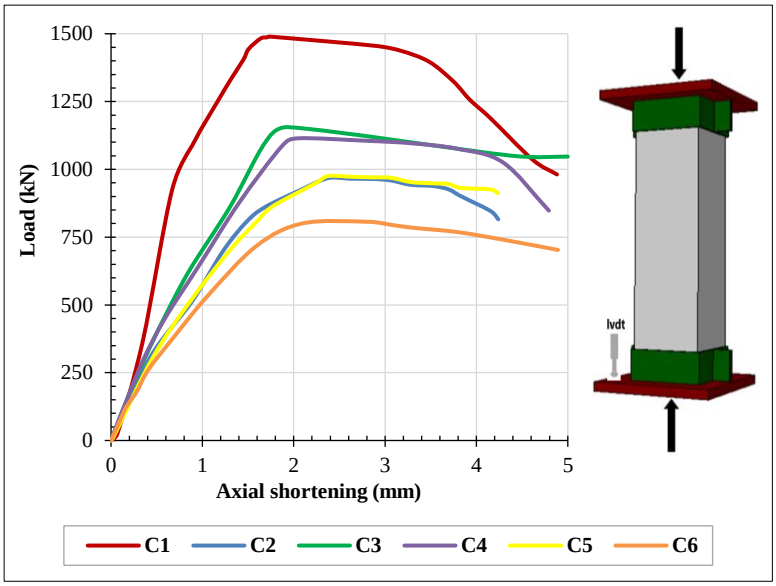

Figure 3. The load-axial shortening curves for tested columns

Figure 4 shows a simplified plot of the axial load-average lateral displacement. The results show that the number of steel tubes, the compressive strength of concrete inside the steel tubes, and the outer compressive strength of concrete increase, with the axial load-lateral displacement relation getting stiffer, exhibiting increased structural stiffness and lower deformation.

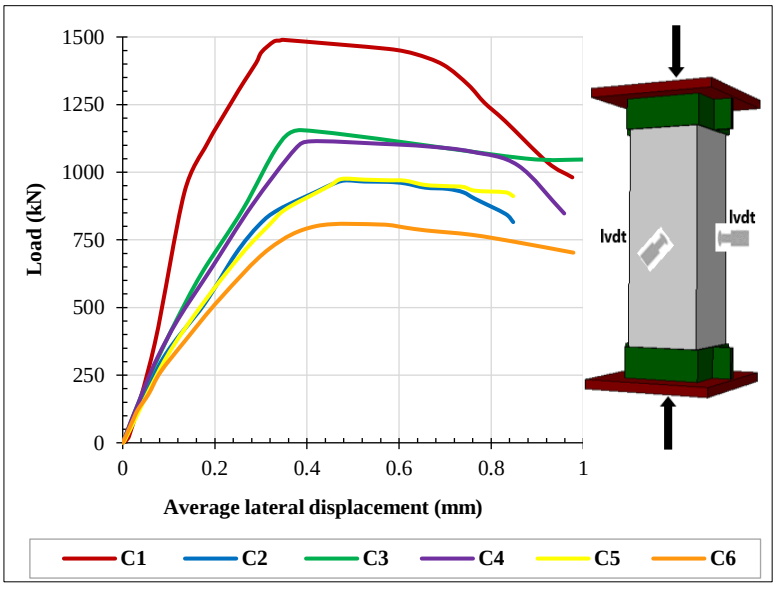

Figure 4. The load-average lateral displacement curves for tested columns

Figures 3 and 4 indicate that the stiffness of the conventional column (C1) is greater than that of the reference column (C2) due to the incorporation of steel rebars. The greater the ratio of CFST, the greater the stiffness in comparison to the

reference column. Additionally, increasing the outer concrete compressive strength also results in greater stiffness in comparison to the reference column. In contrast, an increase in core concrete compressive strength offers the same stiffness to the reference column, whereas an empty steel tube offers lower stiffness compared to the reference column. To investigate the stress at the surface of the concrete at the mid-height of the column, two horizontal strain gauges were utilized in the process of testing on consecutive surfaces at the middle height of the column. In the tests, the strains' readings were recorded at incrementing steps of loading. Figure 5 provides the load-strain graphs at the middle heights of columns that were tested, which provide a hint regarding the nature of deformation of the material under axial compression.

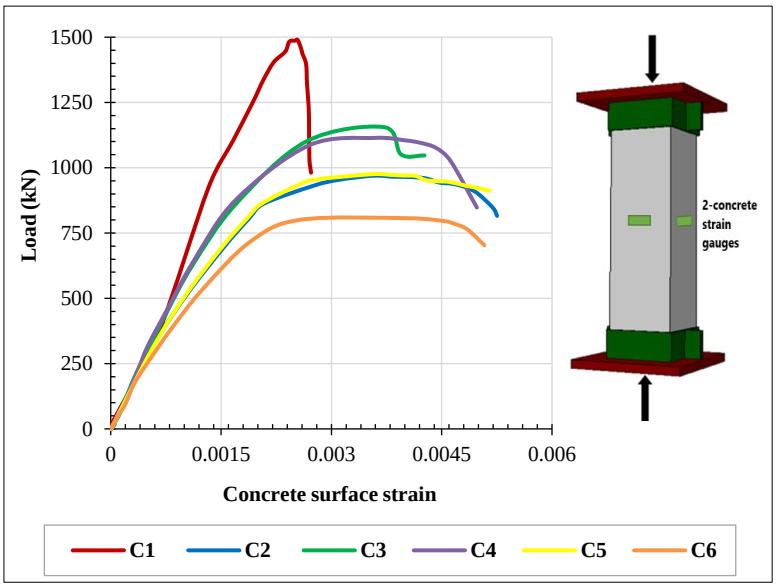

Figure 5. Load-strain behavior for concrete strain gauge in the tested columns

Each of the tested columns is provided with one steel strain gauge on embedded steel tubes. Whereas the conventional column C1 is provided with one steel strain gauge on an embedded reinforcing steel bar. Figure 6 shows the steel tube strain in concrete-encased CFST columns attained yielding, while steel rebar yielded before strain at the conventional concrete column failed. This confirms the ductility of concrete-encased CFST columns.

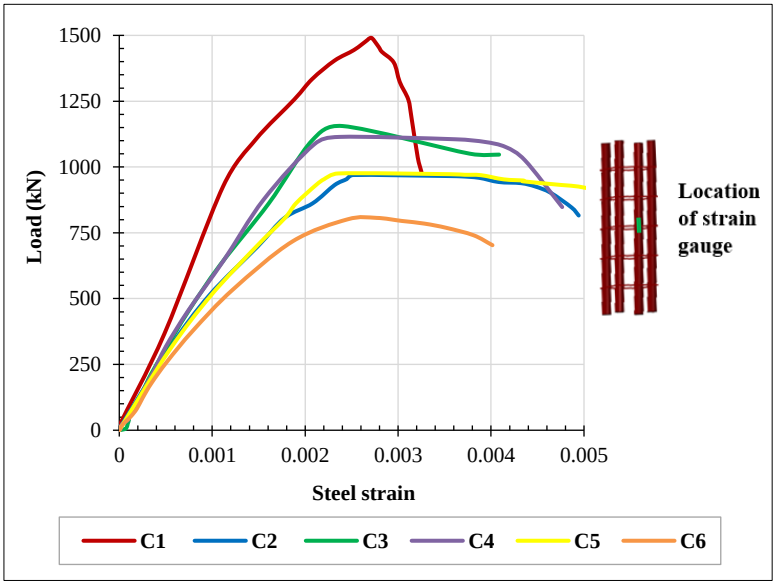

Figure 6. Load-strain behavior for steel strain gauge in the tested columns

The typical column fails principally through concrete crushing and shearing stresses along the sloping planes and outward buckling of longitudinal steel rebar between ties. On the other hand, the failure mode of the concrete-encased CFST column is fundamentally different in the sense that it is a splitting failure mode in addition to yielding of the steel tube, as presented in Figure 7. The difference signifies the superior structural performance of concrete-encased CFST columns in the sense of being more ductile and having a higher ultimate capacity than ordinary columns.

Figure 7. The failure modes of tested columns

4. Finite Element Analysis

The ABAQUS CAE 6.19 software package was employed to employ a finite element method to simulate the performance of concrete-encased CFST columns, as investigated in the experimental research [16, 17].

4.1. Materials Modeling

The Concrete Damage Plasticity (CDP) model is extensively employed as a safe and effective method of concrete behavior simulation under loading. Steel and concrete material stress-strain curves could be utilized to increase the realism in simulation in ABAQUS CAE 6.19. The CDP constitutive model can simulate concrete tensile and compressive failure based on the Lubliner et al. (1989) [18] theory. This model is among the most popular constitutive models for structural analysis. Steel bars and steel tubes, however, are relatively simpler to model with reinforcing behavior compared to concrete. Steel bars and steel tubes are typically assumed to be bilinear in nature for numerical analysis.

4.2. Geometry Modeling

The concrete-encased CFST column is represented as a 3D deformable member with independent outer and inner concrete components. The member was formed by extruding the section in two directions along the third direction. The element employed is C3D8R, an eight-node linear reduced integration brick element. Steel tubes are represented by S4R shell elements, which idealize steel tubes, and lateral steel ties are represented by ductile elements in a 3D system. The T3D2 truss element is a two-node element having x, y, and z directions. The 3D elements of the concrete-encased CFST column were seeded with 20 mm in all three directions [19].

4.3. Verification of Concrete-Encased CFST Columns

Experimental data collected on the reference column (C2) and numerical data are presented in Figure 8. A comparison between real test data and ABAQUS finite element analysis on load-axial shortening curves has been presented in Figure 8. A clear sign was present that the experiment had a high correlation with the finite element analysis and thus confirmed the validity of the simulation.

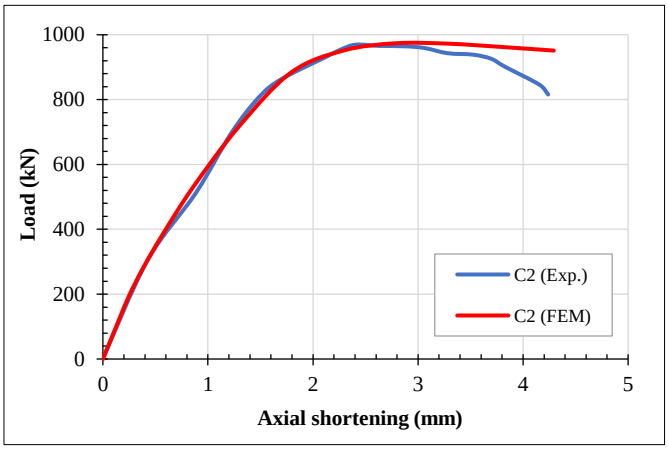

Figure 8. Experimental and ABAQUS load-axial shortening curves

4.4. Parametric Study for Concrete-Encased CFST Columns

The verification numerical modeling was utilized to study all the parameters affecting the axial compression strength of the column. Column C2 was taken as the reference compression specimen. The effect function of each variable was forecasted, as indicated in Figure 9. The findings of the analysis are presented below as follows:

- Axial compressive strength rose from 937.8 to 1858.4 kN with an increase in outer concrete compressive strength from 15 to 45 MPa. The improvement is of the form of a power function with the power being 0.5885.
- Axial strength increased slightly from 947.9 to 984.8 kN with the increase in internal strength from 15 to 45 MPa. This increase is a power function with an exponent of 0.0384.
- Increasing the diameter of the steel tube from 10 to 50 mm enhanced the axial compression strength of the CFST column from 717.9 to 1510.7 kN, with the power function exponent being 0.4544.
- The rising of the yielding stress of the steel tubes from 300 to 800 MPa resulted in a rise of the axial strength of the column from 872.1 to 1185.7 kN, with a power function of 0.3127.
- Axial compressive capacity of the column was enhanced from 954.5 to 1089.8 kN when steel fiber content was enhanced from 0.5 to 2%, while the power function exhibited an exponent value of 0.0941.

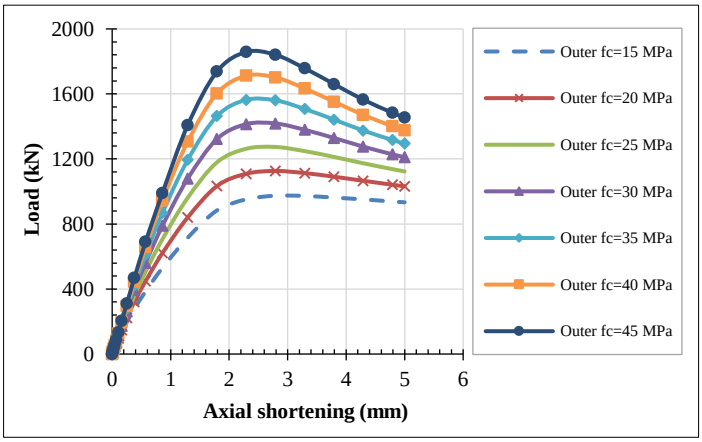

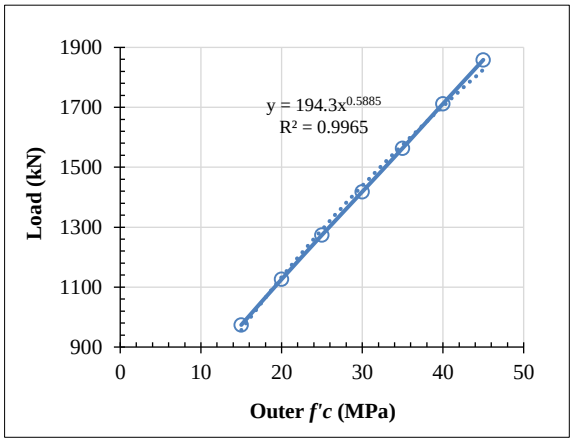

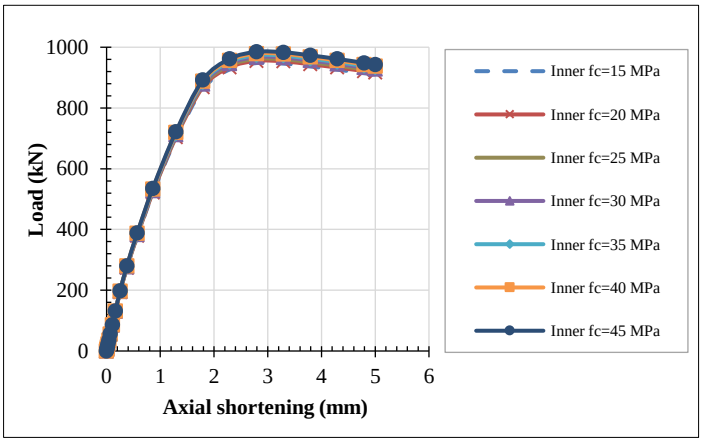

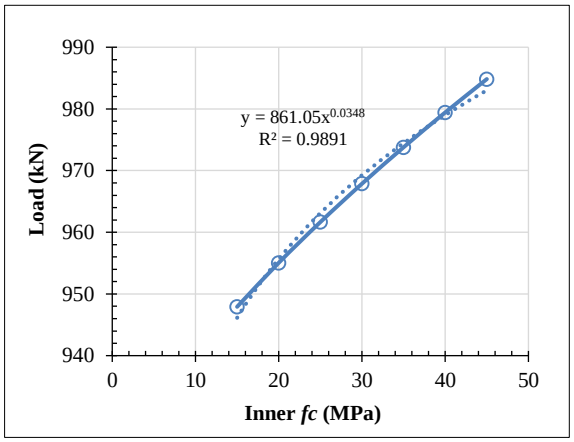

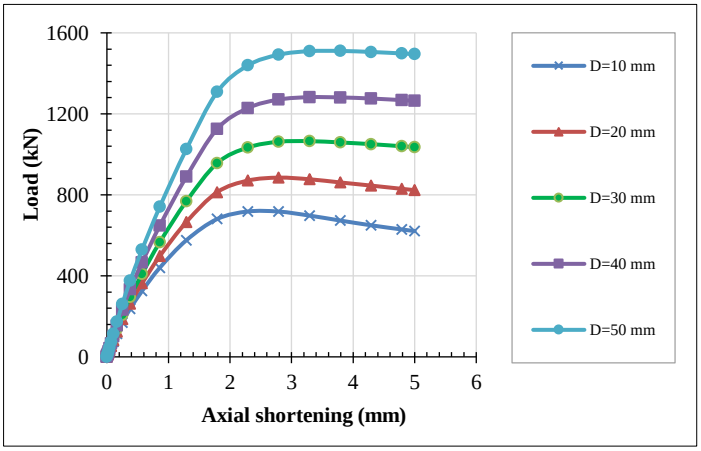

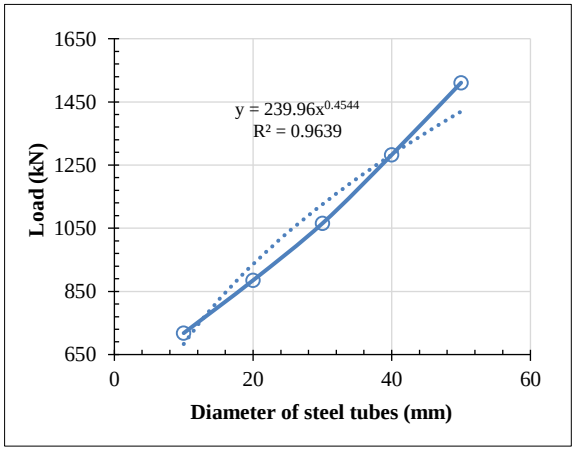

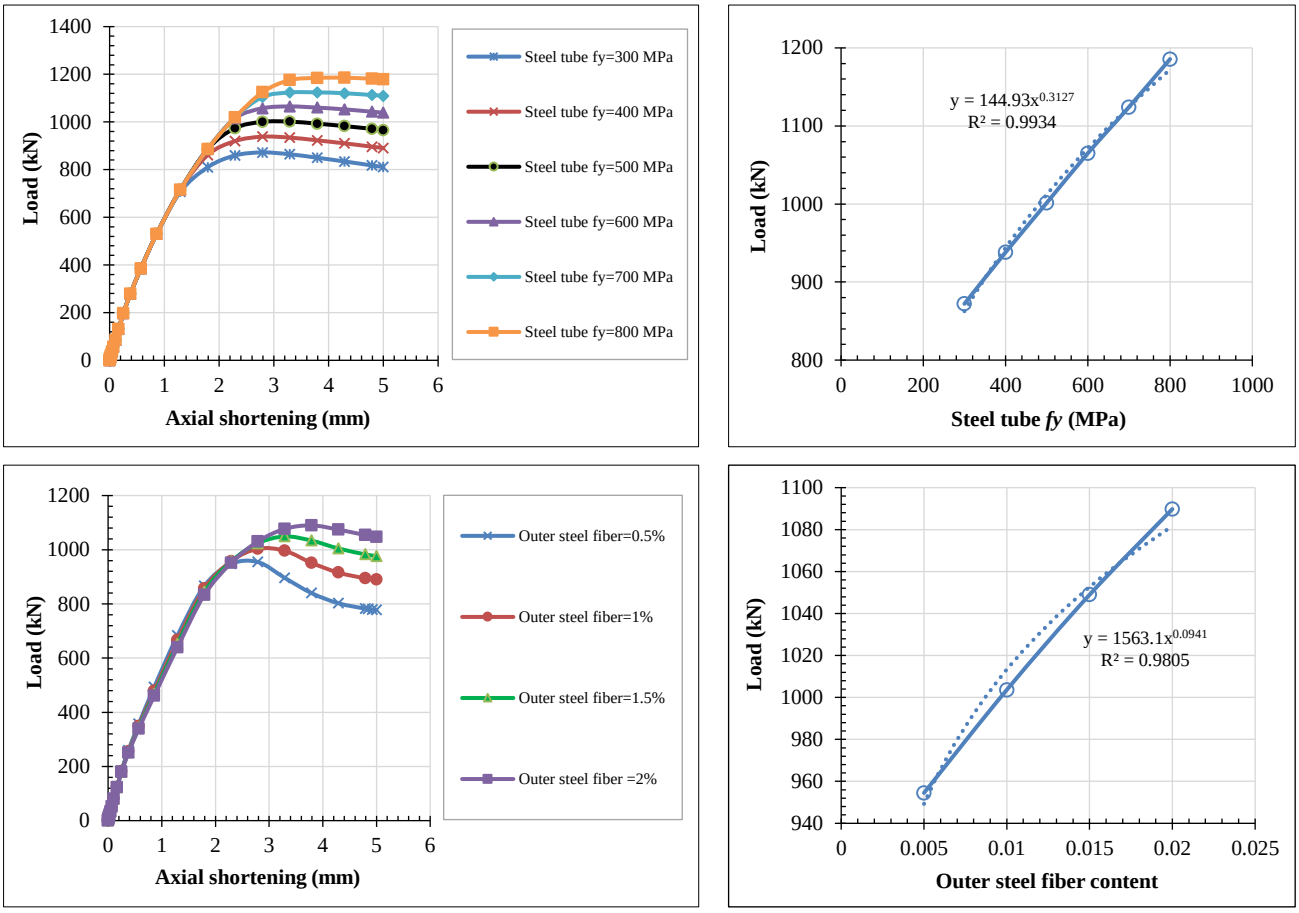

Figure 9. Load-deflection curve and Influence function of parametric study on axial compression strength of concrete-encased CFST column

5. Conclusion

The present study aims to use CFST as the main reinforcement in a short column; therefore, the axial compression strength of the concrete-encased CFST column was 65.1% of that of the conventional column with steel reinforcement. Increasing the ratio of CFST, outer concrete compressive strength, and core strength of concrete on steel tubes increases the axial compression strength of concrete-encased CFST columns. Meanwhile, an unfilled steel tube reduces the axial compression strength of a concrete-encased CFST tube. Through the parametric study in finite element analysis, the behavior of concrete-encased CFST columns exhibiting the highest power function effect at the variables of outer concrete compressive strength, steel tube diameter, and yield stress of steel tubes.

6. Nomenclature

A	Cross-sectional area of concrete-encased CFST	A_{core}	Cross-sectional area of core concrete in CFST
A_s	Cross-sectional area of steel tube in CFST	A_{sc}	Cross-sectional area of CFST (A_{core}+ A_s)
B	Sectional width	CFST	Concrete Filled Steel Tube
CDP	Concrete Damaged Plasticity	e	Load eccentricity
FST	Filled Steel Tube	FEA	Finite Element Analysis
H1	The vertical part of the box's concrete depth of the test SCC	H2	The depth of the concrete at the terminus of the horizontal segment of the box of test SCC
f_c	Concrete cylinder compressive strength	LVDT	Linear Variable Differential Transformer
NC	Normal concrete	P_u	Ultimate load
Ratio of CFST	Cross section area of CFST over gross sectional area of outer concrete	SCC	Self-Compacted Concrete
w/c	Water to cement ratio	λ	Slenderness ratio
ϕ	Diameter of steel tube or steel rebar		

7. Declarations

7.1. Author Contributions

Conceptualization, R.A. and H.A.; methodology, R.A. and H.A.; software, R.A. and M.E.; validation, R.A., H.A., and M.E.; formal analysis, R.A. and M.E.; investigation, R.A. and H.A.; resources, R.A. and M.E.; data curation, R.A. and H.A.; writing—original draft preparation, R.A. and H.A.; writing—review and editing and submitting, R.A., H.A., and M.E. All authors have read and agreed to the published version of the manuscript.

7.2. Data Availability Statement

The data presented in this study are available in the article.

7.3. Funding

The authors received no financial support for the research, authorship, and/or publication of this article.

7.4. Conflicts of Interest

The authors declare no conflict of interest.

8. References

[1] Han, L. H., & An, Y. F. (2014). Performance of concrete-encased CFST stub columns under axial compression. Journal of Constructional Steel Research, 93, 62–76. doi:10.1016/j.jcsr.2013.10.019.

[2] An, Y. F., Han, L. H., & Zhao, X. L. (2014). Analytical behaviour of eccentrically loaded concrete encased CFST box columns. Magazine of Concrete Research, 66(15), 789–808. doi:10.1680/macr.13.00330.

[3] Ali, A. A., Abdul-Sahib, W. S., & Sadik, S. N. (2013). Experimental behavior of circular steel tubular columns filled with self-compacting concrete under concentric load. Engineering and Technology Journal, 31(14), 2760-2772.

[4] An, Y. F., & Han, L. H. (2014). Behaviour of concrete-encased CFST columns under combined compression and bending. Journal of Constructional Steel Research, 101, 314–330. doi:10.1016/j.jcsr.2014.06.002.

[5] Chen, J. Y., Li, W., Han, L. H., Wang, F. C., & Mu, T. M. (2019). Structural behaviour of concrete-encased CFST box stub columns under axial compression. Journal of Constructional Steel Research, 158, 248–262. doi:10.1016/j.jcsr.2019.03.021.

[6] Ali, A. A., & Abbas, N. J. (2021). Behavior of Box Concrete-Filled Steel Tube Columns Considering Confinement Effect. International Journal of Steel Structures, 21(3), 950–968. doi:10.1007/s13296-021-00483-0.

[7] Al-Abbas, B., Abdul Rasoul, Z. M. R., Hasan, D., & Rasheed, S. E. (2023). Experimental Study on Ultimate Strength of Steel Tube Column Filled with Reactive Powder Concrete. Civil Engineering Journal (Iran), 9(6), 1344–1355. doi:10.28991/CEJ-2023-09-06-04.

[8] Abdulkhudhur, R., Al-Quraishi, H., & Elwi, M. (2024). Numerical analysis of concrete-encased concrete filled steel tube beams. AIP Conference Proceedings, 3219(1), 0236329. doi:10.1063/5.0236329.

[9] Al-Khazaleh, M., Kumar, P. K., Qtiashat, D., & Alqatawna, A. (2024). Experimental Study on Strength and Performance of Foamed Concrete with Glass Powder and Zeolite. Civil Engineering Journal, 10(12), 3911-3925. doi:10.28991/CEJ-2024-010-12-06.

[10] Al-Quraishi, H., Kammash, K. N. A., & Abdul-Husain, Z. A. (2022). Bond Strength Behavior in Rubberized Concrete. International Journal of Sustainable Construction Engineering and Technology, 13(1), 130–136. doi:10.30880/ijscet.2022.13.01.012.

[11] Abdulkhudhur, R., Al-Quraishi, H., & Abdullah, O. H. (2020). Effect of steel fiber on the shear transfer strength across a crack in reactive powder concrete. IOP Conference Series: Materials Science and Engineering, 737(1), 012001. doi:10.1088/1757-899X/737/1/012001.

[12] EFNARC. (2002). Specification and Guidelines for Self-Compacting Concrete. Association House, Chicago, United States.

[13] BS EN, 12350-8. (2010). Testing fresh concrete - Part 8: Self-compacting concrete -Slump-flow test. British Standards Institute (BSI), London, United Kingdom.

[14] BS EN, 12350-10. (2010). Testing fresh concrete - Part 10: Self-compacting concrete – L box test. British Standards Institute (BSI), London, United Kingdom.

[15] BS EN, 12350-9. (2010). Testing fresh concrete - Part 9: Self-compacting concrete — V-funnel test. British Standards Institute (BSI), London, United Kingdom.

[16] Al-Quraishi, H., Al-Farttoosi, M., & Abdulkhudhur, R. (2019). Compression Splices of Reinforcing Bars in Reactive Powder Concrete. Civil Engineering Journal, 5(10), 2221–2232. doi:10.28991/cej-2019-03091406.

[17] Mawlood, D., & Rafiq, S. (2022). Nonlinear 3D Finite Element Model for Round Composite Columns under Various Eccentricity Loads. Engineering and Technology Journal, 40(11), 1605–1614. doi:10.30684/etj.2022.133106.1168.

[18] Lubliner, J., Oliver, J., Oller, S., & Oñate, E. (1989). A plastic-damage model for concrete. International Journal of Solids and Structures, 25(3), 299–326. doi:10.1016/0020-7683(89)90050-4.

[19] Abdulkhudhur, R., Lafta, M. J., & Al-Quraishi, H. (2024). Estimation the flexural-tensile strength of fiber reinforced concrete members. AIP Conference Proceedings, 2864(1), 50005. doi:10.1063/5.0186183.